Magnetic Antidot Arrays With a Storage Density of 10 Gbits/cm^2

Z. L. Xiao*, Catherine Y. Han, U. Welp, H. H. Wang, G. A. Willing, V. K. Vlasko-Vlasov, W. K. Kwok, D. J. Miller, J. M. Hiller, R. E. Cook, and G. W. Crabtree

Materials Science Division, Argonne National Laboratory, Argonne, Illinois 60439
*Corresponding author, email: xiao@anl.gov

ABSTRACT

We report a new way to fabricate ultrahigh density storage media by forming magnetic antidot arrays through the deposition of magnetic materials on substrates containing nanopore arrays. In this work, membranes of aluminum oxide that contain lattices of uniform nanopores formed during the anodization of aluminum foils in acids were utilized as deposition substrates. Nickel antidot arrays with density up to 10^{10}/cm^2 have been fabricated by depositing nickel onto these anodic aluminum oxide membranes. Microscopy images show a high degree of order in the antidot arrays. Various sizes and shapes of the antidots were observed with increasing thickness of the deposited nickel. New features appear in both the magnetization and transport measurements when the external magnetic field is parallel to the current direction on these antidot arrays, including an enhancement and a nonmonotonous field dependence of the magnetoresistance, larger value of the coercive field, and a smaller saturation field.

Keywords: Storage media, magnetic antidots, nickel films, anodic aluminum oxide, nanopore arrays.

1 INTRODUCTION

Recently, a new generation of ultrahigh density magnetic storage media has attracted much attention. Promising candidates include arrays of magnetic nanowires [1], self-assembled magnetic nanoparticles [2], magnetic dots [3,4] and antidots [5-12]. In the latter case, antidots are believed to have advantages over dots [5]. First of all, there is no superparamagnetic lower limit to the bit size because there is no isolated volume; the stability of the written bits increases with increasing storage density in the antidot array rather than remaining unchanged as in the dot array. Although the antidot array can be formed by self-assembly during film deposition [6] or annealing of films after fabrication [7], a common and more controllable method is to pattern the films using electron-beam lithography [5,8-11] or focused ion beam milling [12]. Submicrometer antidots have been demonstrated using these advanced techniques. Here we present a convenient way to fabricate ultrahigh density magnetic antidots with sizes down to 20 nm by depositing magnetic materials on substrates with highly ordered arrays of nanopores. The magnetic antidot arrays were characterized using field emission scanning electron microscopy (FESEM), transmission electron microscopy (TEM), as well as magnetization and magnetoresistance measurements.

2 EXPERIMENTAL DETAILS

There are a few types of commercially available membranes containing arrays of nanopores, e.g. nuclear track-etched mica [13] and polycarbonates [14]. Due to the totally disordered distribution of the nanopores, however, they are not suitable in applications such as magnetic recording, which requires that exact position of the storage bits be located in a predictable manner. Recently, progress has been made in achieving highly ordered nanopore arrays in diblock copolymer [15] and anodic aluminum oxide (AAO) [16] membranes. The latter is more popular due to the simple fabrication and the excellent uniformity in diameter and spacing of the pores. In this research we used AAO membranes as substrates to fabricate ultrahigh density magnetic antidot arrays.

AAO membranes were fabricated by anodizing aluminum foils in acidic solutions. Arrays of pores of various diameters and spacings can form under appropriate anodization conditions [16]. Our AAO membranes were fabricated by a two-step anodization procedure as described previously [16]. The starting materials were aluminum foils with dimensions of 20×30×0.5 mm^3. In order to achieve a surface with a roughness in the range of a few nanometers, the foils were first electropolished in a mixed solution of perchloric acid and ethanol (1:8) for 10 minutes at a current density of 200-500 mA/cm^2. The first anodization was carried out in a 0.3M oxalic acid solution at 0°C by applying a constant voltage of 40 V for 24 hours. The resulting alumina layer was then removed by immersing the specimen in a mixture of phosphoric acid (6wt%) and chromic acid (1.8wt%) at room temperature. This procedure leaves a highly ordered array of dimples on the aluminum surface that initializes the pore array formation in the following anodization. The second anodization was carried out under the same condition as the first one. After the second anodization AAO membranes with highly ordered arrays of nanopores were obtained by removing the unreacted aluminum in a saturated $HgCl_2$ or 0.1 M $CuCl_2$ solutions. The diameter of the as-grown pores, as shown in Fig.1, is about 40 nm and can be enlarged by immersing AAO membranes in phosphoric acid (5wt%). Because the size of the magnetic antidots is related to the stability of the

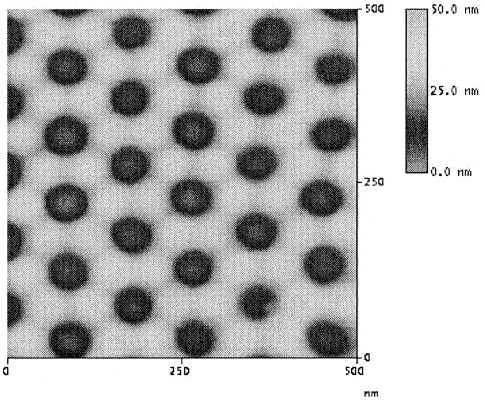

Fig.1. AFM image of the nanopore array in an AAO membrane.

written bits, we fabricated antidots of various sizes with the same density by depositing layers of magnetic material of various thicknesses on membranes with a pore size of about 70 nm.

The magnetic antidots were prepared by depositing nickel (Ni) onto AAO membranes at room temperature by DC magnetron sputtering. The base vacuum was better than 10^{-4} Pa. High purity argon was used as working gas at a pressure of 2.5-3.0 Pa. The deposition rate was about 10 nm/min. Reference Ni-films were deposited onto glass substrates concurrently with the Ni/AAO samples.

3 RESULTS AND DISCUSSION

Figure 1 shows an atomic force microscope (AFM) image of a typical pore array in an AAO membrane anodized at 40 V. The uniformity of the pore diameter and the high degree of order of the array can be seen. The spacing between the centers of the pores is about 100 nm. This corresponds to a density of pores of ~10^{10}/cm^2 or a storage density of 10 Gbits/cm^2 for magnetic antidot arrays, more than 100 times denser than that reported in Ref.12.

Inspection by FESEM reveals that the shape and size of the antidots changed with increasing thickness of the deposited nickel. When the nickel layer was thin (5 nm) the antidots retained the same shape and size as the pores in the AAO membrane. With increasing thickness of the nickel, the size of the holes was reduced and the shape of the holes became hexagonal at a nickel thickness of about 40-50 nm [see Fig.2]. Further increase of the nickel thickness to 100 nm resulted in an irregular hole shape [see Fig.3(a)] with a approximate diameter of 20 nm. The holes are finally closed and a continuous film formed at a thickness of about 200 nm. Figure 3 (b) shows the cross section of the 100 nm thick antidot array at 45 degree angle relative to surface of the membrane. It shows that the antidots indeed have an open bottom and their size decreases gradually towards the top surface. These results demonstrate a highly controllable method varying the size

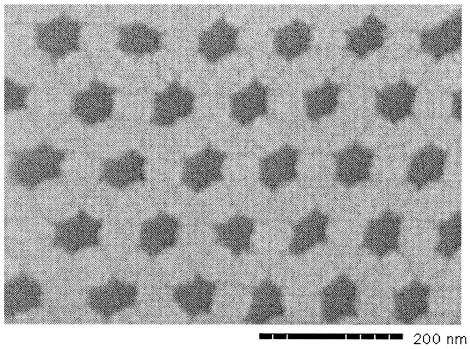

Fig.2. SEM image of a 50 nm thick nickel antidot array.

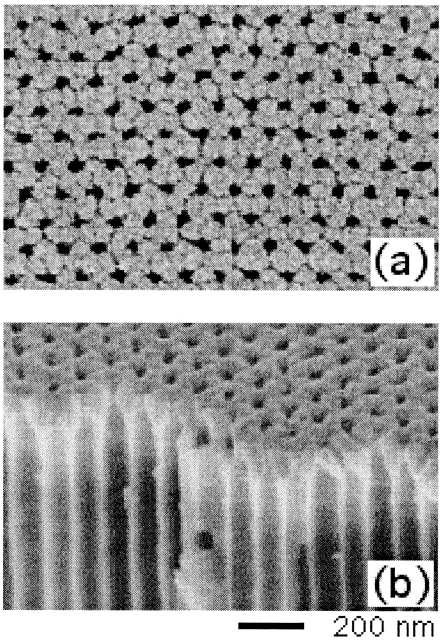

Fig.3. SEM images of a 100 nm thick nickel antidot array: (a) top view and (b) cross section view.

and shape of the antidots, which have important effects on the stability of the written bits [5]. TEM images reveal that the nickel antidots are polycrystalline with an average grain size of about 10-15 nm. Dark-field TEM shows that there is no preferential grain alignment.

The magneto-transport and magnetization data for the 100 nm thick films are summarized in Figs. 4 and 5, respectively. The magnetic field was applied in the film plane either parallel or perpendicular to the current direction, yielding the longitudinal and transverse magnetoresistance, respectively. The continuous film is characterized by an almost reversible magnetization (Fig.5) which is essentially the same for both orientations and approaches saturation near 0.15 Tesla, and by a monotonous negative magnetoresistance, MR = $R(H)/R(0)$-1 [Fig.4(a)]. The

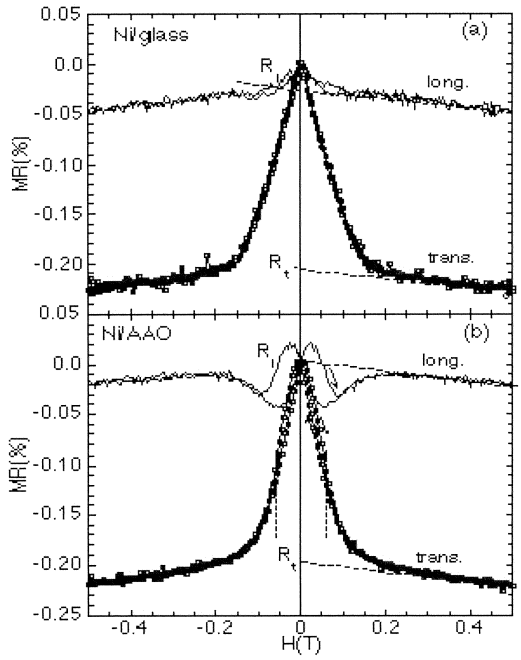

Fig.4. Field dependence of longitudinal magneto-resistances. (a) reference film (Ni/glass) and (b) nickel antidot array (Ni/AAO) with a thickness of 100 nm. The measurements were carried out at a temperature of 280 K. The magnetoresistance MR is defined as: MR=$R(H)/R(0)$-1.

magneto-transport data can be accounted for in the frame-work of conventional anisotropic magnetoresistance (AMR) [17] in which an anisotropic spin-orbit coupling induces maximum resistance when the magnetic moments are aligned parallel to the current direction and a minimum resistance for perpendicular alignment. The AMR can be described by $R=R_t+(R_l-R_t)\cos^2(\phi)$ [17]. Here, R_t and R_l are the transverse and longitudinal resistance interpolated to H=0 as shown in Fig.4, and ϕ is the angle between magnetization and current. The AMR ratio $(R_l - R_t)/R(H=0)\approx 0.2\%$ is reduced as compared to values in bulk samples [18]. There may be several reasons for this observation. In constrained geometries such as thin films or thin wires the magnetoresistance is suppressed due to scattering at the sample surfaces [18]. In addition, due to the polycrystalline nature of the samples field independent contributions to the resistivity arising from grain-boundary scattering reduce the AMR ratio. A weak, almost linear and orientation independent magnetoresistance occurs in fields well above saturation. Similar behavior is frequently observed and is attributed to the suppression of spin-scattering [19].

The magnetization curve of the antidot array exhibits a loop with enhanced values of coercive field (0.006T) and remnant magnetic moment (see Fig.5). We attribute these changes to the interplay of shape anisotropy introduced by holes and inhomogeneous magnetization rotation caused by the nanoscale patterning of the magnetic film. For bulk Ni the domain wall width is $\delta = \pi (A/K)^{1/2} \approx 125$ nm with the exchange constant $A=8\times10^{-7}$ erg/cm [20] and the anisotropy constant $K= 5\times10^4$ erg/cm^3 [21]. In samples composed of non-textured nanoscale grains the effective anisotropy is strongly reduced [22] as compared to the bulk value and δ is enhanced. Thus, in the patterned Ni-films studied here the effective domain wall width is substantially larger than the bridges between the holes and, hence the nucleation and propagation of magnetic domain walls is not expected. The magnetization process then occurs through the inhomo-geneous rotation of the magnetic moments. One could also expect that the magnetoelastic anisotropy, which is introduced by the film/substrate lattice mismatch and is usually essential in Ni films due to large magnetostriction coefficients [23] should be less in the antidot array due to the large free surface. A lower saturation field H_s for the antidot array compared to the continuous film in Fig.5 supports such a suggestion. In addition, the magnetostatic energy, $2\pi M_s^2$, associated with the large internal surfaces induces the preferential alignment of the magnetic moments parallel to the hole circumference giving rise to the enhanced low-field magnetization hysteresis (Fig.5).

The magneto-transport data of the patterned 100 nm thick Ni-film is shown in Fig. 4(b). The hysteretic behavior, particularly in the longitudinal resistivity com-ponent, is clearly seen. Whereas the transverse magneto-resistance shows similar over-all behavior and magnitude as seen in the continuous film, unusual non-monotonic behavior is observed in the longitudinal magnetoresistance which we attribute to the inhomo-geneous rotation of the magnetic moments with respect to the applied field and current directions. Since the remnant moment is small in low magnetic fields, the magnetic moments point in all directions. However, the moments as well as the current

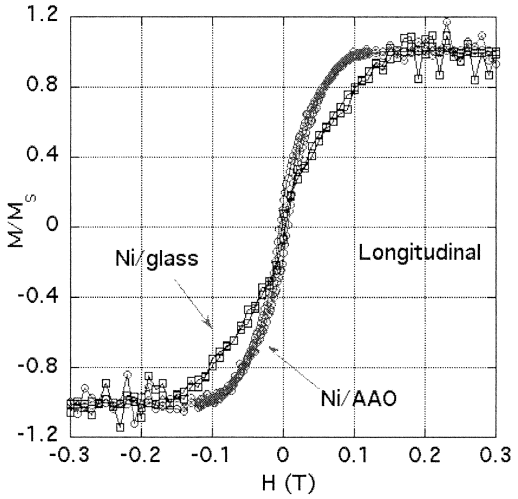

Fig.5. Field dependence of the magnetization of a nickel antidot array (Ni/AAO) with a thickness of 100 nm. Results of its reference film are also shown for comparison.

trajectories, conform to the hole array. Therefore, locally, current and magnetization are largely parallel or antiparallel resulting in an enhanced longitudinal AMR. With increasing field the magnetic moments inhomogeneously and irreversibly rotate towards the field direction whereas the current flow pattern does not change. Transverse components of the magnetization (with respect to the current direction) arise, causing the observed decrease in the resistivity. With further increase of fields, these transverse components decrease again and the magnetoresistance increases. Correspondingly, in the transverse resistance (the average current direction is perpendicular to the field) the magnetization components are essentially parallel to the current and contribute to a higher resistance. Superimposed on the steep field dependence a shoulder near 0.06 Tesla [marked by the vertical dotted lines in Fig. 4(b)] signals this effect, which is then suppressed with increasing field, in good agreement with the longitudinal data.

4 SUMMARY

In summary, we demonstrated an attractive way to achieve ultrahigh density recording media by depositing magnetic layers onto substrates with arrays of ultrahigh density nanopores. Arrays of nickel antidots on porous anodic aluminum oxide membranes show high degree of order and adjustability of the size and shape of the antidots. New features in the field dependence of the magnetization and magnetoresistance indicate opportunities of interesting new physics in nanoscale antidot arrays.

5 ACKNOWLEDGMENT

This work was supported by the US Department of Energy (DOE), BES-Materials Science, Contract No. W-31-109-ENG-38. The FESEM imaging was performed in the Electron Microscopy Center of Argonne National Laboratory.

REFERENCES

[1] T. M. Whitney, J. S. Jiang, P. C. Searson, C. L. Chien, Science, **261**, 1316 (1993); A. Fert and L. Piraux, J. Magn. Magn. Mater. **200**, 338 (1999); A. J. Yin, J. Li, W. Jian, A. J. Bennett, and J. M. Xu, Appl. Phys. Lett. **79**, 1039 (2001).

[2] S. H. Sun, C. B. Murray, D. Weller, L. Folks, A. Moseral, Science **287**, 1989 (2000).

[3] D. D. Awschalon and D. P. DiVincenzo, Phys. Today **48**, 43 (1995).

[4] For a review see R. P. Cowburn, J. Phys. D: Appl. Phys. **33**, R1-R16 (2000).

[5] R. P. Cowburn, A. O. Adeyeye, and J. A. C. Bland, Appl. Phys. Lett. **70**, 2309 (1997); A. O. Adeyeye, J. A. C. Bland, C. Daboo, *ibid* **70**, 3164 (1997).

[6] Chengtao Yu, Dongqi Li, J. Pearson, and S. D. Bader, Appl. Phys. Lett. **78**, 1228 (2001).

[7] H. Shi and D. Lederman, J. Appl. Phys. **87**, 6095 (2000).

[8] Y. Otani, S. G. Kim, T. Kohda, and K. Fukamichi, IEEE Trans. Magn. **34**, 1090 (1998).

[9] C. T. Yu, H. Jiang, L. Shen, P. J. Flanders, and G. J. Mankey, J. Appl. Phys. **87**, 6322 (2000).

[10] I. Guedes, N. J. Zaluzec, M. Grimsditch, V. Metlushko, P. Vavassori, B. Ilic, P. Neuzil, and R. Kumar, Phys. Rev. B **62**, 11719 (2000).

[11] U. Welp, V. K. Vlasko-Vlasov, G. W. Crabtree, Carol Thompson, V. Metlushko, and B. Ilic, Appl. Phys. Lett. **79**, 1315 (2001).

[12] A. Yu. Toporov, R. M. Langford, and A. K. Petford-Long, Appl. Phys. Lett. **77**, 3063 (2000).

[13] L. Sun, P. C. Searson, and C. L. Chien, Appl. Phys. Lett. **74**, 2803 (1999).

[14] L. Piraux, J. M. George, J. F. Despres, C. Leroy, E. Ferain, R. Legras, K. Ounadjela, and A. Fert, Appl. Phys. Lett. **65**, 2484 (1995); A. Blondel, J. P. Meier, B. Doudin, and J. -Ph. Ansermet, *ibid* **65**, 3019 (1995).

[15] T. Thurn-Albrecht, J. Schotter, G. A. Kästle, N. Emley, T. Shibauchi, L. Krusin-Elbaum, K. Guarini, C. T. Black, M. T. Tuominen, and T. P. Russell1, Science **290**, 2126 (2000).

[16] H. Masuda and K. Fukuda Science **268**, 146 (1995); H. Masuda and M. Satoh, Jpn. J. Appl. Phys. **35**, L120 (1996).

[17] T. R. McGuire and R. I. Potter, IEEE Trans. Magn. **11**, 1018 (1975).

[18] T. G. S. M. Rijks, R. Coehoorn, M. J. M. de Jong, and W. J. M. de Jonge, Phys. Rev. B **51**, 283 (1995).

[19] I. A. Cambell, A. Fert "Transport Properties of Ferromagnets" in *Ferromagnetic Materials*, Vol 3, ed. E. P. Wohlfarth (North Holland, Amsterdam, 1992); A. O. Adeyeye, G. Lauhoff, J. A. C. Bland, C. Daboo, D. G. Hasko, and H. Ahmed, Appl. Phys. Lett. **70**, 1046 (1997); Y. Wu, Y. Suzuki, U. Rüdiger, J. Yu, A. D. Kent, T. K. Nath, and C. B. Eom, Appl. Phys. Lett. **75**, 2295 (1999).

[20] A. T. Aldred, Phys. Rev. B **11**, 2597 (1975).

[21] W. Gong, H. Li, Z. R. Zhao, and J. C. Chen, J. Appl. Phys. **69**, 5119 (1991).

[22] G. Herzer, J. Magn. Mag. Mat. **112**, 258 (1992); J. F. Loeffler, H.-B. Braun, and W. Wagner, Phys. Rev. Lett. **85**, 1990 (2000).

[23] E. Kloholm and J. Aboaf, J. Appl. Phys. **53**, 2661 (1982).